

# LY2603618, a selective CHK1 inhibitor, enhances the anti-tumor effect of gemcitabine in xenograft tumor models

Darlene Barnard<sup>1</sup> · H. Bruce Diaz<sup>1</sup> · Teresa Burke<sup>1</sup> · Gregory Donoho<sup>1</sup> · Richard Beckmann<sup>1</sup> · Bonita Jones<sup>1</sup> · David Barda<sup>1</sup> · Constance King<sup>1</sup> · Mark Marshall<sup>1</sup>

Received: 23 September 2015 / Accepted: 16 November 2015 / Published online: 27 November 2015  
© Springer Science+Business Media New York 2015

**Summary** Pharmacological inhibition of CHK1 in the absence of p53 functionality leads to abrogation of the S and G2/M DNA damage checkpoints. We report the preclinical therapeutic activity of LY2603618 (CHK1 inhibitor) at inhibiting CHK1 activation by gemcitabine and enhancing *in vivo* efficacy. The *in vivo* biochemical effects of CHK1 inhibition in the absence or presence of DNA damage were measured in human tumor xenograft models. Colon, lung and pancreatic xenografts models were treated with gemcitabine, LY2603618, or gemcitabine plus LY2603618. Gemcitabine treatment alone induced a significant increase in CHK1 autophosphorylation over untreated tumors. Co-administration of LY2603618 with gemcitabine showed a clear inhibition of CHK1 autophosphorylation for at least 24 h. Combining LY2603618 with gemcitabine resulted in an increase in H2AX serine 139 phosphorylation, indicating a corresponding increase in damaged DNA in the tumors. LY2603618 abrogated the S-phase DNA damage checkpoint in Calu-6 xenograft tumors treated with gemcitabine but did not significantly alter the G2/M checkpoint. Combining gemcitabine with LY2603618 resulted in a significant increase in tumor growth inhibition in Calu-6, HT-29 and PAXF 1869 xenografts over gemcitabine treatment alone. The best combination efficacy occurred when LY2603618 was given 24 h following dosing with gemcitabine. LY2603618 worked effectively to remove the S-phase DNA damage checkpoint and increase the DNA damage and the antitumor activity of gemcitabine treatment.

**Keywords** LY2603618 · CHK1 · DNA-damage · Gemcitabine · Xenograft

## Introduction

Interference with DNA damage checkpoints has been demonstrated to be an effective means of increasing the cytotoxicity of a number of DNA-damaging cancer therapies in preclinical experiments. Cell cycle arrest at these checkpoints protects injured cells from apoptotic cell death until DNA damage can be repaired. In the absence of functioning checkpoints, cells with damaged DNA may proceed into premature mitosis followed by cell death. A highly complex and networked response, the pre-mitotic DNA damage checkpoints can be separated into the G1/S, intra-S and G2/M checkpoints, each with critical control proteins [1]. An essential regulator for both the G1/S and G2/M checkpoints is the p53 tumor suppressor protein [2]. As a transcriptional regulator, p53 is responsible for maintaining a durable checkpoint rather than triggering an immediate arrest in response to DNA damage. In TP53 mutant tumor cells the G1/S checkpoint is absent and the G2/M checkpoint abbreviated. A key protein kinase required for the rapid activation and maintenance of the S and G2/M checkpoints is Checkpoint Kinase 1 or CHK1 [3]. Independent of p53, the CHK1 protein coordinates cellular responses to the most common types of DNA damage [4]. Single-stranded DNA breaks or stalled replication forks are the primary activators of the CHK1 pathway. Once activated, CHK1 suppresses the S phase and M phase cyclin-dependent kinases via Cdc25 destabilization [3]. Rapid loss of CDK activity stalls the cell cycle during DNA replication and prior to entry into mitosis, providing the cell with time to repair DNA damage. If the damage is too extensive, the cell will die through

✉ Mark Marshall  
mmarshall@lilly.com

<sup>1</sup> Lilly Research Laboratories, Eli Lilly and Company, Indianapolis, IN 46285, USA

apoptosis. In the absence of functioning p53, CHK1 becomes the primary mediator of DNA damage checkpoint control.

Gemcitabine (2'-deoxy-2',2'-difluorocytidine monohydrochloride), a nucleoside analogue commonly used in the treatment of solid tumors, is an effective DNA damaging agent [5]. A prodrug, gemcitabine is metabolized by intracellular nucleoside kinases sequentially into dFdCDP and dFdCTP. Each of these compounds has a unique target and effect which contributes to the cytotoxic action of gemcitabine. dFdCDP inhibits ribonucleotide reductase resulting in reduced levels of deoxyribonucleotides available for DNA synthesis. dFdCTP is competitive with dCTP for incorporation into replicating DNA. With a reduction in intracellular dCTP, dFdCTP is effectively incorporated into growing DNA chains, resulting in chain termination. Repair enzymes are unable to efficiently remove the gemcitabine nucleotide and the replication fork collapses causing severe replication stress [6]. This leads to activation of the CHK1-dependent DNA damage checkpoints, arrest of cells in S-phase and eventually breaks at the stalled replication forks.

The idea of improving response to DNA damaging therapies through the inhibition of critical checkpoint regulators is over 20 years old [7]. Originally identified as a checkpoint regulator in fission yeast [8], CHK1 is a conserved regulator of DNA damage response in vertebrates as well. Loss of CHK1 function by genetic knockout, RNAi knockdown or small molecule inhibitors has been repeatedly demonstrated to sensitize cells to most methods of damaging DNA, particularly in the presence of TP53 mutations [9]. Since the majority of human cancers lack fully functioning p53, interfering with CHK1 control of checkpoints provides a unique opportunity to selectively increase the effectiveness of DNA damaging chemotherapy [10]. Chemical inhibition of CHK1 and the corresponding loss of the DNA damage checkpoints results in increased DNA strand breakage following gemcitabine treatment [11]. This may be a consequence of both forced cell cycle progression with diminished DNA damage repair and replication catastrophe brought on by extended exposure of single-stranded DNA at the collapsed forks. Replication catastrophe refers to massive double stranded DNA breaks that can occur as a result of inhibiting ATR or CHK1 during conditions of replication stress [12, 13].

A number of small molecule inhibitors of CHK1 have been developed for clinical use. The majority of these CHK1 inhibitors demonstrated preclinical activity when co-administered with DNA damaging therapeutics and some have advanced into phase 1 and 2 trials. Unfortunately, in spite of signs of clinical efficacy, most CHK1 inhibitors have been discontinued from clinical trials because of toxicity, pharmacokinetics or business reasons [13]. As of this writing only GDC-0575 (NCT0156425) and LY23606368

(NCT02124148, NCT02514603, NCT02203513, NCT02555644) are in active clinical trials. CCT245737 and V-158411 have been declared as intended for clinical development [14, 15]. One of the first selective CHK1 inhibitors to enter clinical development was LY2603618 [16]. LY2603618 is a highly selective inhibitor of CHK1 and objective responses were observed in Phase 1 assessments in combination with both pemetrexed, pemetrexed/cisplatin and gemcitabine [16–18]. Although the development of LY2603618 was recently discontinued, understanding the preclinical activity and mechanism of action of LY2603618 remains of value, particularly as new CHK1 inhibitors continue to enter and advance in the clinic. In this study we report the mechanism and activity of LY2603618 in combination with the antimitabolite drug gemcitabine in human xenograft models for NSCLC, colorectal cancer, and pancreatic cancer.

## Materials and methods

### Cell culture

HT-29 colon cancer cells and Calu-6 non-small cell lung cancer cells were from American Type Culture Collection (ATCC), Manassas, VA. PAXF 1869 human pancreatic cancer tumor cells were maintained as xenografts by serial passage in nude mice (Oncotest GmbH) [19].

### Antibodies

This study used the following antibodies: phospho-histone H3 serine 10 or pH3 (S10) (Millipore 06–570), phospho-CHK1 serine 296 or pCHK1 (S296) and phospho-CHK1 serine 345 or pCHK1 (S345) (Cell Signaling Technology 2349 and 2341), phospho-Histone H2.AX serine 139 or pH2A.X (S139) (Millipore 05–636), ribonucleotide reductase subunit R2 or RRM2 (Santa Cruz Biotechnology SC10846), donkey anti-rabbit HRP, sheep anti-mouse HRP (Amersham NA934V and NA9310V), and donkey anti-goat HRP (Santa Cruz Technology SC2020).

Immunoblotting of proteins was as previously described [20]. Immunoblot band intensity was determined using a LAS-4000 imaging system (FUJIFILM Corp) and quantified using TotalLab™ gel analysis software (Nonlinear Dynamics LTD).

### Compounds and compound preparation

LY2603618 was formulated for oral dosing as a solution in 16.66 % Captisol® (CyDex Inc) in 25 mM phosphate buffer, pH 4, and stored at 4 °C until use. Gemcitabine hydrochloride

(Eli Lilly and Company or Qventas) was prepared in saline for intraperitoneal *in vivo* dosing or in water for *in vitro* use.

### Tumor xenograft CHK1 inhibition models

The biochemical activity of LY2603618 in treated xenograft tumors was determined by immunoblotting for pCHK1 (S296) as described elsewhere [20]. To initiate tumor growth, athymic nude mice (Harlan Laboratories) were irradiated within 24 h of implant with 450 rads total body irradiation. Animals were implanted subcutaneously with  $1 \times 10^6$  cells for Calu-6. Animal treatment commenced once the tumor implants reached approximately 150 mm<sup>3</sup>. The duration of drug treatment varied according to the experiment and is described in the figure legends. For combination studies, all animals received equal numbers of injections using either compounds or vehicles [20]. Following treatment, tumors were removed and prepared for analysis as previously described [20]. Statistical analyses were performed in JMP (SAS). *p*-values were calculated by One-Way ANOVA, with Dunnett's post-test used to compare treatment groups to appropriate control groups.

### Tumor xenograft efficacy models

Tumor growth delay studies using the HT-29 and Calu-6 cell lines, conducted at ICOS, utilized female Balb/c nu/nu mice (Charles River Laboratories). The tumor growth inhibition studies with the HT-29 cell line were run at Lilly Research Laboratories using female athymic nu/nu mice (Harlan). To initiate tumor growth, animals were implanted subcutaneously with  $5 \times 10^6$  cells. The tumor growth inhibition study with the PAXF 1869 patient derived xenograft was performed at Oncotest GmbH using female NMRI nu/nu mice (Harlan). Tumors were initiated by cutting harvested xenograft tumors into 4–5 mm fragments which were implanted subcutaneously in anesthetized mice. Dosing was begun when tumors reached a mean volume of 100–150 mm<sup>3</sup>. The dose of each drug and the schedule followed are described in the figure legends for each experiment. Maximum tolerated dose for gemcitabine was as previously determined [21]. Animals that showed >20 % weight loss or other severe symptoms were sacrificed. Tumor xenograft studies followed each institution's animal care and use guidelines.

Efficacy data analysis was performed with the SAS statistical analysis program (SAS Institute; versions 8.2 and 9.1), as described [17]. Tumor growth inhibition was calculated by setting the first measurement following the conclusion of dosing as the reference point for inhibition, and defining the 100 % tumor growth inhibition level as the mean baseline tumor volume recorded on the day of animal randomization,

which occurred either on or immediately preceding the first day of dosing.

### High content cell imaging

High content cell imaging and analysis was performed using the Cellomics Arrayscan Vti using a 10x objective fluorescent detector (Cellomics) [22]. Cells (2500–5000 per well) were plated in 96 well poly D-lysine coated black clear bottom plates (BD Biocoat). Following an appropriate experimental time period, the cells were formaldehyde fixed, permeabilized, then blocked with BSA and stained according to figure legends. Hoechst 33342 was purchased from Molecular Probes. TUNEL assay was performed using the *in situ* cell death detection kit purchased from Roche Diagnostics. Subsequent images were analyzed using the Cellomics Target Activation BioApplication. All fluorescent intensities are displayed as relative fluorescent units.

### DNA sequencing

Exome sequencing was performed on an Illumina HiSeq 2000 starting from 3ug of DNA using the SureSelect Human All Exon v1 (38 Mb) protocol (Agilent). Paired-end sequencing with read length of 100 base pairs and 80X average on-target coverage was achieved. Reads were mapped to the human genome build 37 (hg19) using the Burrows-Wheeler Aligner (BWA) [23] and variants were called with SAMtools [24], Genome Analysis Toolkit (GATK-lite version) [25] and FreeBayes [26].

Sanger sequencing was used to confirm CHEK2 deletion identified by exome sequencing. PCR and sequencing primers are as follows; PCR\_CHK2\_F1: AAAGGAAGAATTTGCACTCTGG, PCR\_CHK2\_R1: GAACTATAGGTCTGGGC TGTTAGG, Sanger\_CHK2\_F2: GCCTATGATCCGTCCA TTCTAGG, Sanger\_CHK2\_R2: CTTGAAACTCACCTTT GTTGTGG. PCR was cycled at 95 °C for 2 min; 35 cycles of 95 °C for 30 s; 68 °C for 30 s, 72 °C for 30 s, and a final extension of 72 °C for 10 min. The purified PCR products were sequenced using an ABI 3730xl DNA analyzer. All sequences were visually analyzed with Mutation Surveyor DNA variant analysis software (v.3.97 Softgenetics).

## Results

### Gemcitabine causes rapid and sustained activation of DNA damage responses

Prior to testing LY2603618 as a chemopotentiator for gemcitabine, we first modeled the *in vitro* cell cycle effects of gemcitabine treatment in the TP53<sup>R196\*</sup> mutant Calu-6 lung carcinoma cell line. Although gemcitabine has been used as

clinical agent since 2006, the effects of the compound on the cell cycle have not been extensively studied under conditions mimicking clinical drug exposure. Typically, gemcitabine has been characterized *in vitro* using 24–96 h exposure to the prodrug. The half-life of gemcitabine in patients following short <70 min infusions ranges from 32 to 94 min. The half-life of gemcitabine triphosphate in cells is much longer, up to 12 h [27]. To better match the clinical pharmacokinetics of a 30 min infusion, cultured cells were treated with a ‘bolus’ of 100 nM gemcitabine for 2 h followed by washout of the drug [28]. At 12, 24 and 36 h following gemcitabine washout, the cells were fixed to the culture plates and analyzed by high content imaging for cell number and DNA content (Fig. 1). Twelve hours following the drug washout, there was a large increase in G1/early S-phase cells with a corresponding decrease in the G2/M populations. By 24 and 36 h, the S-phase population had more than doubled in both lines with a corresponding loss of G1 cells. By 36 h the percentage of cells in the G2/M peak had returned to or greater than control levels. A reduction in phosphorylation on histone H3 serine 10 indicated that the 36 h G2/M peak consisted of cells primarily in late S and G2-phase, not mitosis (Table 1). A small pH3+ mitotic population continued to persist, perhaps reflecting impairment of the G2/M checkpoint in the absence of functioning p53. As expected following gemcitabine treatment, there was a large increase in the number of cells with positive staining for the DNA damage marker pH2AX (S139).

The *in vivo* effects of gemcitabine were also determined using Calu-6 tumor xenografts. Mice bearing Calu-6 tumor xenografts were dosed once with 30, 60 or 150 mpk gemcitabine. The tumors were removed either 4 or 8 h after

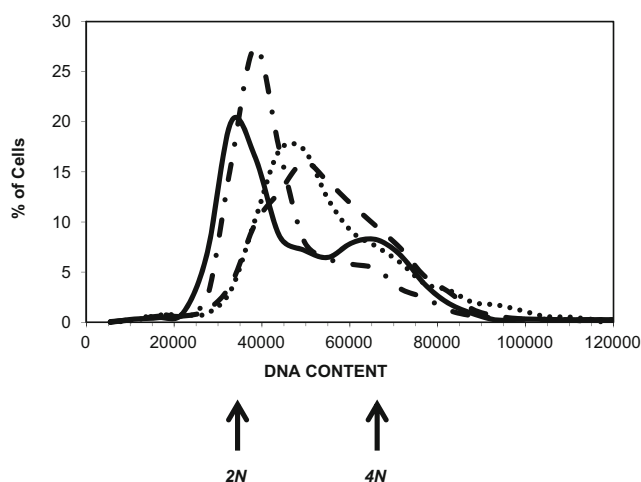


**Fig. 1** Pulsed gemcitabine treatment causes a sustained S/G2 arrest *in vitro*. Calu-6 cells were treated with 100 nM gemcitabine for 2 h followed by drug washout. Cells were grown for an additional 12, 24 or 36 h and analyzed for DNA content, dsDNA damage (pH2AX (S139)) and mitosis (pH3 (S10)) by high content image analysis. The peaks designating 2 N (G1) and 4 N (G2/M) cell populations are denoted by arrows. No gemcitabine (—); 12 h (•••••); 24 h (—•—•—); 36 h (—•—•—)

**Table 1** Gemcitabine treatment causes a sustained S/G2 arrest *in vitro*

	DMSO 36 h.	Gem 36 h.
% 2 N (G1)	58.5	22.1
% >2 N <4 N (S)	15.5	37
% 4 N (G2/M)	26	40.9
% pH3+ / 4 N+ (M)*	2.6	0.5
% pH2AX+ *	5	50.3
pH2AX (X±SD)	842±361	1529±510

Cells were treated with 100 nM gemcitabine for 2 h followed by drug washout. The fraction of cells in each phase of the cell cycle for each treatment group was calculated from high content image data of cells stained by Hoechst dye and antibodies for pH3 (S10) and pH2AX (S139) as described in the Fig. 1 legend

\*Positive cut-off based on value >95 % of DMSO control cells

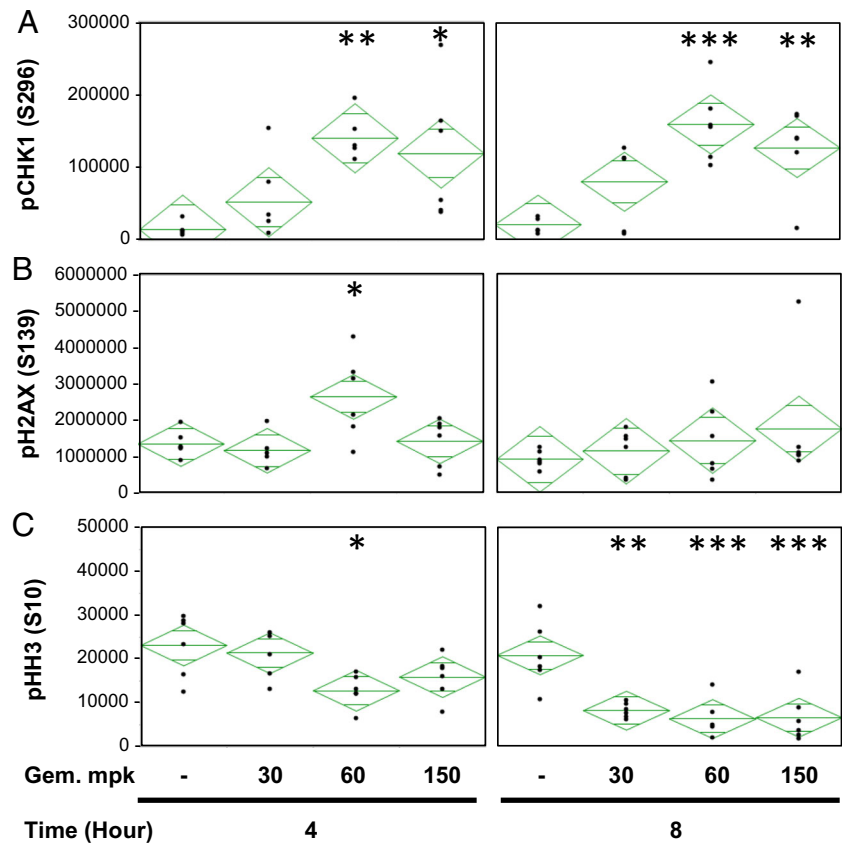
gemcitabine treatment and processed for immunoblot analysis with antibodies specific for DNA damage (pH2AX Ser139), DNA damage checkpoint activation (pCHK1 Ser296) and mitosis (pH3 Ser10) [20]. In spite of a shorter time between treatment and analysis, gemcitabine caused cell cycle changes in the tumors nearly identical to those observed *in vitro* (Fig. 2a, b, c). After 4 h, significant activation of CHK1 was observed for both the 60 and 150 mpk treatment groups. However, significant DNA damage and decreased mitosis was only significant in the 4 h, 60 mpk group. Eight hours following gemcitabine treatment, the Calu-6 tumors continued to show significant activation of CHK1 in the 60 and 150 mpk groups with significant loss of mitotic cells at all three drug concentrations. There was no significant increase in DNA damage in Calu-6 tumors in the 8 h 150 mpk group. Furthermore, loss of mitotic cells was much more easily detected than was CHK1 activation and DNA damage. This likely reflects that replication collapse caused by gemcitabine is a potent inducer of the replication checkpoint event without large amounts of DNA damage.

#### LY2603618 inhibits activation of CHK1 by gemcitabine, increases DNA damage and abrogates the S-phase checkpoint in Calu-6 tumor xenografts

Prior to testing the *in vivo* effectiveness of combining LY2603618 with gemcitabine, the dose of LY2603618 required to effectively inhibit activated CHK1 was determined. Calu-6 xenografts were selected for this experiment due to the more robust CHK1 activation observed following gemcitabine treatment. Mice bearing Calu-6 xenografts were treated with 150 mg/kg gemcitabine followed 6 h later with varied oral doses of LY2603618. Tumors were removed 2 h following LY2603618 administration, processed and the extracts analyzed by immunoblot for CHK1 serine 296



**Fig. 2** Gemcitabine activates CHK1 and blocks mitotic progression *in vivo*. Mice bearing Calu-6 ( $n=6$ ) xenograft tumors were dosed once with 30, 60 or 150 mg/kg gemcitabine. Tumors were removed either 4 or 8 h later, processed and analyzed by immunoblot for the following phosphoproteins: (a) pCHK1 (S296), (b) pH2A.X (S139) and (c) pH3 (S10). Significance was calculated relative to the no gemcitabine control groups. Unmarked ( $p>0.05$ ); \* 0.01  $<p<0.05$ ; \*\*0.001  $<p<0.01$ ; \*\*\* $p<0.001$



autophosphorylation. The  $ED_{50}$  for inhibition of gemcitabine-induced CHK1 autophosphorylation was calculated to be 21.3 mpk with nearly 100 % inhibition occurring at 200 mpk (Fig. 3).

In order to assess the effects on DNA damage response resulting from combining LY2603618 with gemcitabine, mice implanted with Calu-6 tumor xenografts were administered vehicle, 150 mg/kg gemcitabine, 200 mg/kg LY2603618 or

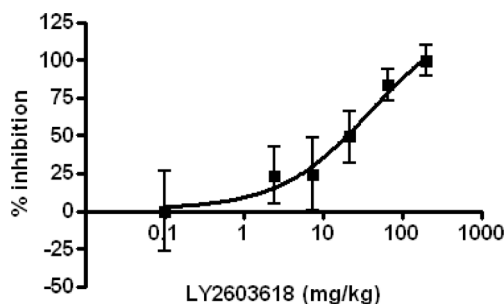


**Fig. 3** LY2603618 dose response for inhibition of gemcitabine activation of CHK1 autophosphorylation. Mice bearing Calu-6 xenograft tumors were dosed with gemcitabine for 6 h followed by increasing doses of LY2603618. Two hours after LY2603618 was administered the tumors were removed for processing and blood drawn to measure drug exposure. Autophosphorylation of CHK1 on serine 296 was measured in the lysates by immunoblotting and the relative value determined for each LY2603618 treatment group was converted into percent inhibition of the pCHK1 (S296) signal induced by gemcitabine alone

gemcitabine plus LY2603618 concurrently. Tumors were removed either 8 or 24 h later and analyzed by immunoblot for phosphorylation of CHK1 serine 345 by ATR, CHK1 serine 296 autophosphorylation and H2AX serine 139 phosphorylation (Fig. 4a, b, c; also see [20]). Although activated by gemcitabine at both 8 and 24 h, CHK1 activity is strongly inhibited by co-administration of LY2603618 for at least 24 h. As shown previously, LY2603618 did not inhibit the phosphorylation of CHK1 on serine 345 by ATR [20]. CHK1 serine 345 phosphorylation increased after 8 h of combination treatment as described previously for other CHK1 inhibitors [29]. In this xenograft model, treatment with gemcitabine alone caused minimal double-stranded DNA breaks as indicated by no increase in pH2AX (S139) levels. However when gemcitabine and LY2603618 are combined, a two-fold increase in pH2AX (S139) was measured in as little as 8 h and further increased nearly four-fold by 24 h, indicating an accumulation of DNA damage in the tumors.

The same Calu-6 xenograft tumors were also used to ascertain the effect of LY2603618 on the DNA damage checkpoints activated by gemcitabine treatment (Fig. 4d, e). As a DNA replication inhibitor, gemcitabine treatment induces the S-phase DNA damage checkpoint [30]. This can be measured in tumors as an increase in the R2 subunit of ribonucleotide reductase (RRM2), an S phase marker [31], and a decrease in mitotic phosphorylation of histone H3 on serine 10. Although

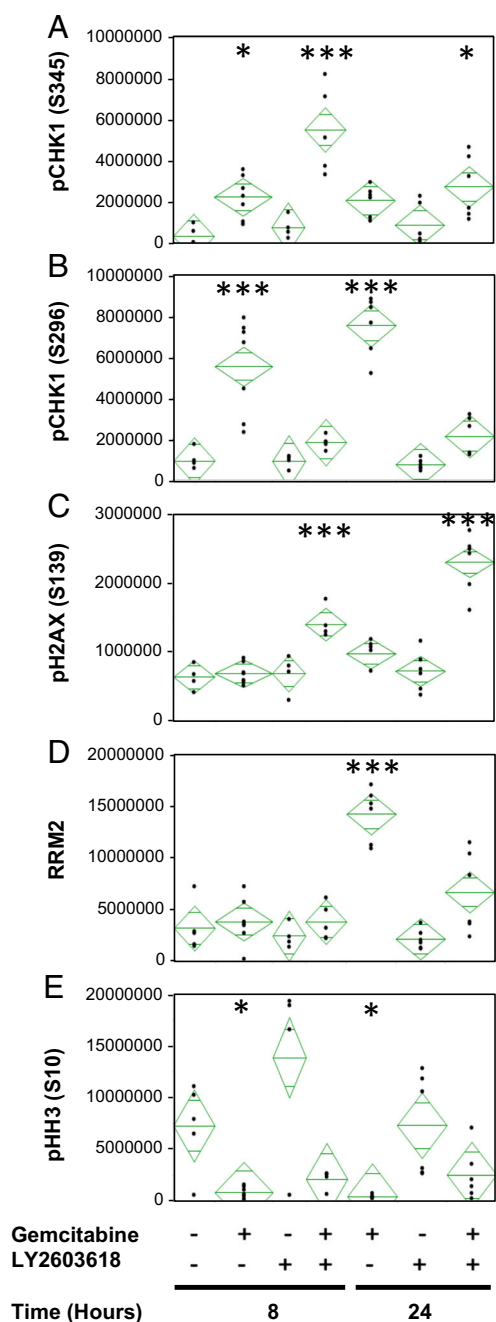


**Fig. 4** A single dose of LY2603618 inhibits gemcitabine activation of the CHK1 DNA damage response for 24 h. Mice implanted with Calu-6 tumor xenografts were administered vehicle, 150 mg/kg gemcitabine, 200 mg/kg LY2603618 or gemcitabine+LY2603618. Vehicle treated tumors were removed 8 h later and all other treatment groups at 8 and 24 h. Tumors were processed and analyzed by immunoblot for (a) pCHK1 (S345), (b) pCHK1 (S296), (c) pH2AX (S139), (d) RRM2 and (e) pHH3 (S10).  $N=4-7$  animals. Significance was calculated relative to the 8 h no treatment control groups. Unmarked ( $p>0.05$ ); \*  $0.01<p<0.05$ ; \*\* $0.001<p<0.01$ ; \*\*\* $p<0.001$

no changes in the quantity of RRM2 was found after 8 h of treatment with gemcitabine, 24 h of treatment caused a 4-fold increase in the S-phase marker. RRM2 was reduced when

LY2603618 was co-administered with gemcitabine suggesting loss of the replication checkpoint. The number of pHH3+ mitotic cells was dramatically reduced by gemcitabine at both 8 and 24-h treatment times supportive of a premitotic arrest. Tumors treated with both gemcitabine and LY2603618 showed a small, but statistically insignificant increase ( $p>0.05$ ) in H3 phosphorylation relative to gemcitabine alone at 24 h. LY2603618 alone increased the average level of pHH3 (S10) after 8 h, but the increase was not statistically significant compared to the vehicle treated group ( $p>0.05$ ).

#### LY2603618 enhances the anti-tumor effect of gemcitabine in xenograft tumor models

The results of the *in vivo* biochemistry experiments with LY2603618 in combination with gemcitabine predicted that the combination would have superior efficacy in tumor growth inhibition studies over monotherapy alone. To determine if the combination of LY2603618 and gemcitabine exhibits superior efficacy, three xenograft models were selected: Calu-6 lung carcinoma, HT-29 colon carcinoma and PAXF 1869, a patient-derived pancreatic cancer xenograft. In the first xenograft experiments, a maximum tolerated dose of gemcitabine was given once every 3 days to observe the effect of the combination. Mice with Calu-6 and HT-29 tumor xenografts were treated with vehicle, 150–160 mg/kg gemcitabine, 200 mg/kg LY2603618 or gemcitabine followed 24 h later with 50, 100 or 200 mg/kg of LY2603618. In both Calu-6 and HT-29 models gemcitabine strongly inhibited tumor growth during the dosing period with an eventual recovery of tumor growth once dosing was completed (Fig. 5a, b; Table 2). LY2603618 alone had no effect on tumor growth. Combining 200 mg/kg of LY2603618 with gemcitabine increased the tumor growth delay over gemcitabine only treated mice from 10 to 22 days in the Calu-6 LY2603618 group and from 29 to 48 days in the HT-29 model. These results suggest that including LY2603618 in a clinical regimen of maximally dosed gemcitabine may result in an improved outcome for the patient.

From a mechanistic viewpoint, checkpoint abrogation by LY2603618 would be most optimally applied once the maximum number of tumor cells have arrested in S phase. From the results shown in Fig. 1 this would be approximately 24 h following gemcitabine dosing. However from a convenience point of view, clinicians may prefer to give their patients gemcitabine and LY2603618 during the same office visit. An *in vivo* experiment was conducted that allowed comparison of other dosing schedules in addition to the 24 h offset of LY2603618 from gemcitabine. HT-29 xenografts were treated with gemcitabine, but with LY2603618 dosed 24 h prior to, concurrent with or 24 h after gemcitabine dosing. A significant increase in tumor growth delay relative to gemcitabine alone was only observed when LY2603618 was dosed 24 h

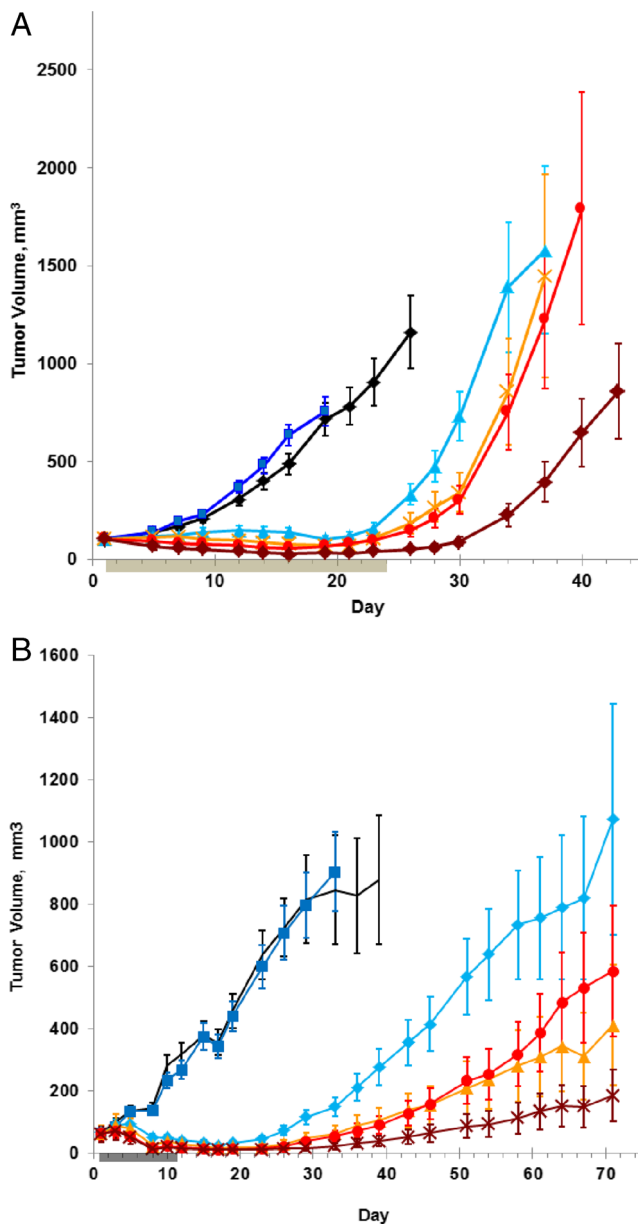


**Fig. 5** LY2603618 Increases Gemcitabine Tumor Growth Delay in Calu-6 and HT-29 Xenograft Tumor Models. **(a)** Calu-6 cells were injected subcutaneously into the flanks of the mice. On the 7th day after implant (assigned to be day 1), animals were randomized into 6 groups of 10 animals and 160 mg/kg Gemcitabine was administered to animals by IP injection. 24 h later animals were administered oral LY2603618. After 1 day of rest, dosing was repeated. In total six cycles of drugs were administered; there was a 1 week rest period between the end of the 4th cycle and start of the 5th cycle. **(b)** HT-29 cells were injected subcutaneously into the flanks of the mice. On the 7th day after implant (assigned to be day 1), animals were randomized into 6 groups of 10 animals and 150 mg/kg Gemcitabine was administered to animals by IP injection. 24 h later animals were administered oral LY2603618. After 1 day rest, dosing was repeated; in total four cycles of drugs were administered. Tumor volumes were measured regularly and the average group tumor volume and standard errors plotted. The time between the first and last dosing days is marked on the x-axis by a bar. Vehicle (—◆—); LY2603618 200 mpk Q3D (d2) (—■—); gemcitabine 160 mpk Q3D (—▲—); gemcitabine Q3D/LY2603618 50 mpk Q3D (d2) (—◇—); gemcitabine Q3D/LY2603618 100 mpk Q3D (d2) (—●—); gemcitabine Q3D/LY2603618 200 mpk Q3D (d2) (—◆—)

gemcitabine or LY2603618 alone, statistical significance relative to the vehicle control group was not achieved. When both agents were combined, tumor growth inhibition was increased over gemcitabine treatment alone. Measured at day 48, the group receiving a single dose of LY2603618 following gemcitabine showed 72 % tumor growth inhibition. The group receiving two consecutive doses of LY2603618 at 24 and 48 h following gemcitabine showed tumor growth inhibition of 78 %. These results indicate that a single dose per cycle of LY2603618 following gemcitabine is sufficient for near maximal potentiation of tumor growth inhibition.

Tumor explants from patients have been shown to be predictive of clinical responsiveness to specific drugs when grown and passaged as tumor xenografts [19]. PAXF 1869 is one such explant from a pancreatic exocrine tumor. Mice implanted with PAXF 1869 were dosed according to a schedule of 100 mg/kg gemcitabine once every 7 days followed 24 h later with 200 mg/kg LY2603618. Dosing was repeated five additional times (Fig. 7). Both gemcitabine and

after gemcitabine (Fig. 6a; Table 3). Tumor growth inhibition for gemcitabine alone was 54.3 %, which was increased to better than 93 % when LY2603618 was combined with a 24 h offset. These results strongly support the need for patients to return to the clinic the day following gemcitabine administration for LY2603618 dosing.

A follow-up experiment addressed the question of whether potentiation of gemcitabine activity by LY2603618 is maximal when LY2603618 is given only once or twice per cycle. Using the HT-29 xenograft model, mice were treated with 60 mg/kg of gemcitabine, a sub-efficacious dose, followed once 24 h or twice 24 and 48 h later by 200 mg/kg LY2603618 for five cycles (Fig. 6b; Table 3). Although tumor growth inhibition trends were observed by 48 days with

**Table 2** Antitumor effects of gemcitabine, LY2603618 alone and in combination with gemcitabine in Calu-6 and HT-29 human xenografts grown in nude mice

Treatment	Tumor Growth Delay in mean days	
	Calu-6 750 mm <sup>3</sup>	HT-29 500 mm <sup>3</sup>
Vehicle	0±1.8	0±3.4
LY2603618 200 mpk	-3±1.5	0±3.2
Gem 160 mpk (Calu-6)	10.3±2.3	
Gem 150 mpk (HT-29)		28.7±4.9
Gem+LY2603618 50 mpk	10.4±2.0	38.3±5.5
Gem+LY2603618 100 mpk	15.1±3.1	39.1±3.3
Gem+LY2603618 200 mpk	21.5±1.9	48.2±5.7

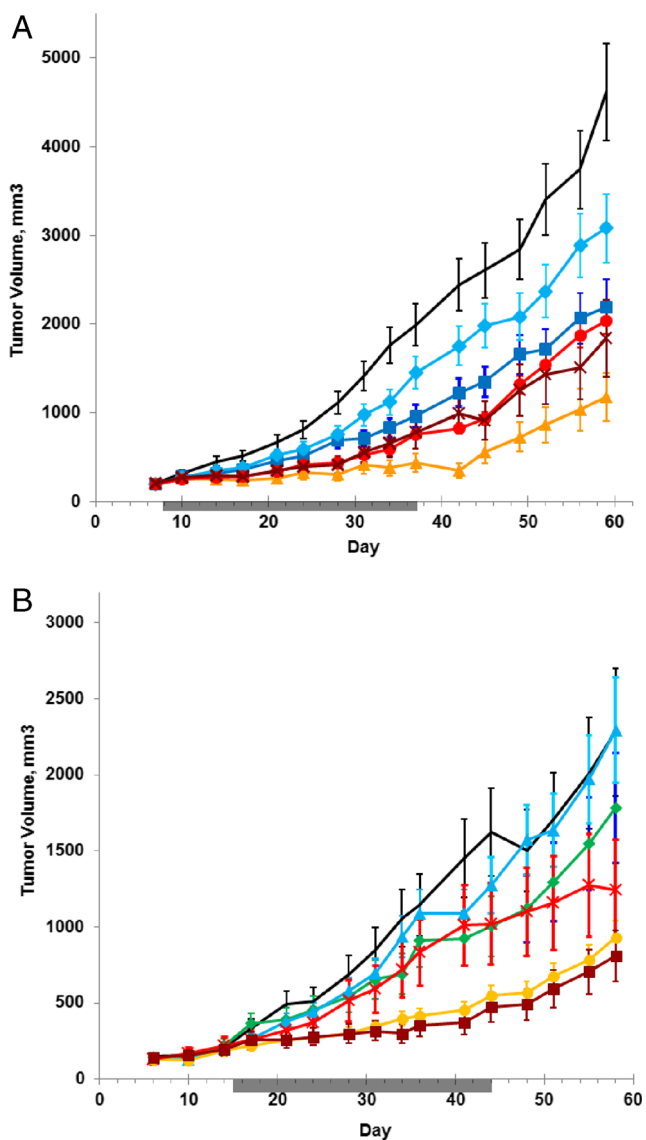


**Fig. 6** A single dose of LY2603618 off-set 24 h from gemcitabine provides maximum tumor growth delay in HT-29 xenograft tumors. **(a)** Mice implanted with HT-29 tumor xenografts were randomized into six groups of eight animals. Groups were dosed according to three different schedules; animals were dosed with 60 mg/kg gemcitabine and 200 mg/kg LY2603618 concurrently, gemcitabine followed 24 h later by LY2603618 or LY2603618 followed 24 h later by gemcitabine. Dosing cycles were repeated weekly; in total five cycles of drugs were administered, so that the last day of dosing was day 37. Vehicle (—); gemcitabine 60 mpk Q7D (■); LY2603618 200 mpk Q7D (d2) (◆); gemcitabine Q7D/LY2603618 Q7D (d2) (▲); gemcitabine Q7D/LY2603618 Q7D (d1) (●); LY2603618 Q7D/gemcitabine Q7D (d2) (×). **(b)** Mice implanted with HT-29 tumor xenografts were randomized into six groups of eight animals. One group was dosed with vehicle and two groups were dosed with 60 mg/kg Gemcitabine. Control and gemcitabine pretreated groups were then dosed with 200 mg/kg LY2603618 according to two schedules; 24 h following gemcitabine or 24 and 48 h following gemcitabine. Dosing cycles were repeated weekly; in total five cycles of drugs were administered. Tumor volumes were measured regularly and the average group tumor volume and standard errors plotted. The time between the first and last dosing days is marked on the x-axis by a bar. Vehicle (—); gemcitabine, 60 mpk Q7D (◆); LY2603618 200 mpk Q7D (d2) (▲); gemcitabine Q7D /LY2603618 200 mpk Q7D (d2) (●); LY2603618 200 mpk Q7D (d2,3) (×); gemcitabine Q7D / LY2603618 200 mpk Q7D (d2,3) (■)

phosphorylated regulatory domain (Fig. 8b). As explained in the discussion, mutation of the CHEK2 gene in PAXF 1869 may help explain the loss of the p53 function necessary to enable LY2603618 potentiation of gemcitabine treatment.

## Discussion

In this study, we report that the inhibition of CHK1 by LY2603618 effectively inhibited activation of CHK1, the S-phase DNA damage checkpoint and increased the extent of DNA damage in gemcitabine-treated tumors. These activities coincide with LY2603618/gemcitabine combination efficacy in three separate human tumor xenograft models.

The concept of interfering with DNA damage checkpoints in human cancer as a means to improve the efficacy of DNA damaging therapies has been demonstrated preclinically with other small molecule inhibitors of CHK1 [33]. An inhibitor of the CHK1 protein kinase, LY2603618 showed excellent selectivity against the majority of the 51 protein kinases tested, including CHK2. Due to its selectivity, LY2603618 treatment induced a cellular phenotype indistinguishable from that resulting from genetic knockdown of CHK1 [34]. LY2603618 effectively neutralized CHK1 activation induced by both gemcitabine and doxorubicin in Calu-6 and HeLa cells *in vitro* and in Calu-6 tumor xenografts [20]. Gemcitabine treatment activates CHK1 as a consequence of stalling the progression of the replication forks, thereby activating the S-phase replication stress checkpoint [35–37].

LY2603618 alone demonstrated minimal efficacy. When combined together, LY2603618 and gemcitabine caused a clear inhibition of tumor growth throughout the period of dosing. Gemcitabine and LY2603618 given as single agents achieved respectively 45 and 28 % tumor growth inhibition while in combination 103 % tumor growth inhibition (regression) was observed. This effect was durable for at least 2 weeks following the completion of dosing. Since *in vivo* activity for the LY2603618/gemcitabine combination has been associated with mutations in TP53 [20, 32] the TP53 gene in PAXF 1869 was sequenced to determine if this correlation was supported. The TP53 gene in PAXF 1869 was found to be wild type. Further examination of the sequence of genes involved in p53 signaling identified a homozygous in-frame five codon deletion in the CHEK2 gene, resulting in the deletion of amino acids 82–86 (DQEPE) (Fig. 8a). The deletion is adjacent to the SQ/TQ region of CHK2 (aa 20–75), a heavily



**Table 3** Antitumor effects of gemcitabine, LY2603618 alone and in combination with gemcitabine in HT-29 human xenografts grown in nude mice. Effects of variation in schedule

Treatment	Tumor Growth Inhibition (%)			
	Order of Addition		Single vs. repeat dosing	
	Day 42	p vs. Gem	Day 48	p vs. Gem
Vehicle Q7D	0±12.9	0.0034	0±20.8	0.2882
Gem 60 mpk Q7D	54.3±7.0		29.3±16.8	
LY2603618 200 mpk Q7D (offset d2)	30.7±9.8	0.1236	-5.4±17.6	0.2136
Gem / LY2603618 (offset d2)	93.3±3.7	<.0001	71.6±5.3	0.0132
Gem / LY2603618 (concurrent)	72.3±2.7	0.0882		
LY2603618 / Gem (offset d2)	65.0±10.2	0.342		
LY2603618 200 mpk Q7D (offset d2,3)			30.8±22.3	0.9036
Gem /LY2603618 (offset d2,3)			77.8±7.8	0.0025

Doxorubicin can interfere with resolution of replicated chromosomes by inhibiting topoisomerase II, ultimately resulting in double-stranded DNA breaks [38].

The CHK1-specific activity demonstrated for LY2603618 *in vitro* was also observed *in vivo*. Using gemcitabine as a DNA damage-inducing treatment, Calu-6 tumor xenografts

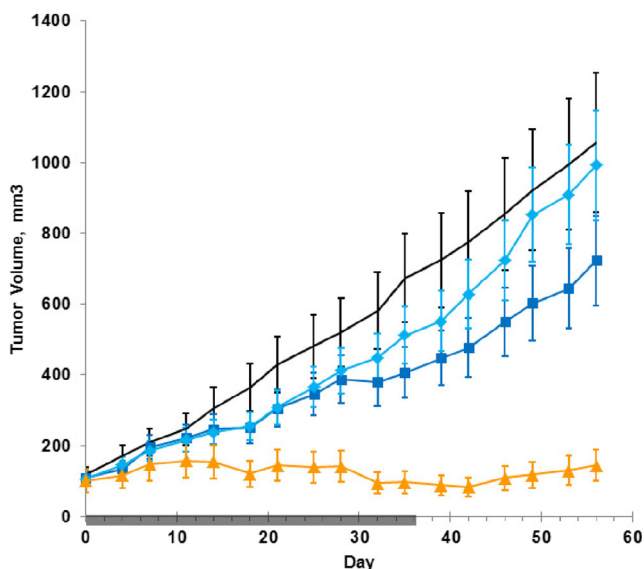


**Fig. 7** LY2603618 enhances the anti-tumor effect of gemcitabine in a PAXF-1869 patient explant tumor model. Tumor fragments from PAXF-1869 pancreatic xenografts were implanted subcutaneously into the flanks of NMRI nude mice and were randomized into four groups of seven or eight animals once the tumors had reached an approximate size of 100 mm<sup>3</sup>. One group was dosed with vehicle and two groups were dosed with 100 mg/kg Gemcitabine. 24 h later the drug-naïve fourth group as well as one of the gemcitabine groups was administered 200 mg/kg LY2603618. The dosing cycle was repeated weekly; in total six cycles of drugs were administered. Tumor volumes were measured regularly and the average group tumor volume and standard errors plotted. Dose groups are as indicated in the figure. The time between the first and last dosing days is marked on the x-axis by a bar. Vehicle (—●—); gemcitabine 100 mpk Q7D (—■—); LY2603618 200 mpk Q7D (d2) (—◆—); gemcitabine Q7D /LY2603618 200 mpk Q7D (d2) (—▲—)

responded by a long lasting induction of the CHK1-dependent checkpoints. Even though the DNA damage marker pH2AX (S139) was only modestly elevated, autophosphorylated CHK1 persisted for at least 24 h. This likely reflects gemcitabine triphosphate (dFdCTP) incorporation into replication origins halting fork progression, but not leading to abundant double-stranded DNA breaks [11]. ATR/CHK1 activation is directly linked to replication stress, which need not include dsDNA breaks [39]. By 24 h, the S-phase marker RRM2 was elevated and the mitotic marker pH3 (S10) reduced, indicative of active S and G2/M checkpoints [31, 40]. When LY2603618 was combined *in vivo* with gemcitabine, CHK1 autophosphorylation was inhibited for at least 24 h and DNA damage was increased at all time points. Decreasing RRM2 in the treated tumors indicated that the S-phase DNA damage checkpoint was rendered at least partially nonfunctional. However, in spite of the absence of functional p53 in Calu-6 cells, the G2/M checkpoint remained intact. This was unexpected since it has been previously demonstrated that combining gemcitabine with a CHK1 inhibitor results in premature mitotic entry by cells with <4 N DNA content, followed by cell death due to chromosome fragmentation [32]. However, the degree of G2/M checkpoint bypass has been shown to be dependent upon the relative concentrations of CHK1 inhibitor and gemcitabine [6]. Synergistic combination of a CHK1 inhibitor and gemcitabine can destabilize the replication apparatus and increase cell killing even when the G2/M checkpoint remains largely unaffected. LY2603618 in combination with gemcitabine did further increased DNA damage in the Calu-6 cells along with releasing the S-phase checkpoint, consistent with potentiation of gemcitabine efficacy *in vivo*.

The primary therapeutic hypothesis for enhancing the efficacy of DNA damaging agents through CHK1 inhibition requires the loss of the DNA damage checkpoints. LY2603618 causes abrogation of the S-phase checkpoint *in vivo* and this activity increased the efficacy of gemcitabine in multiple tumor xenograft models. The Calu-6 model was not as

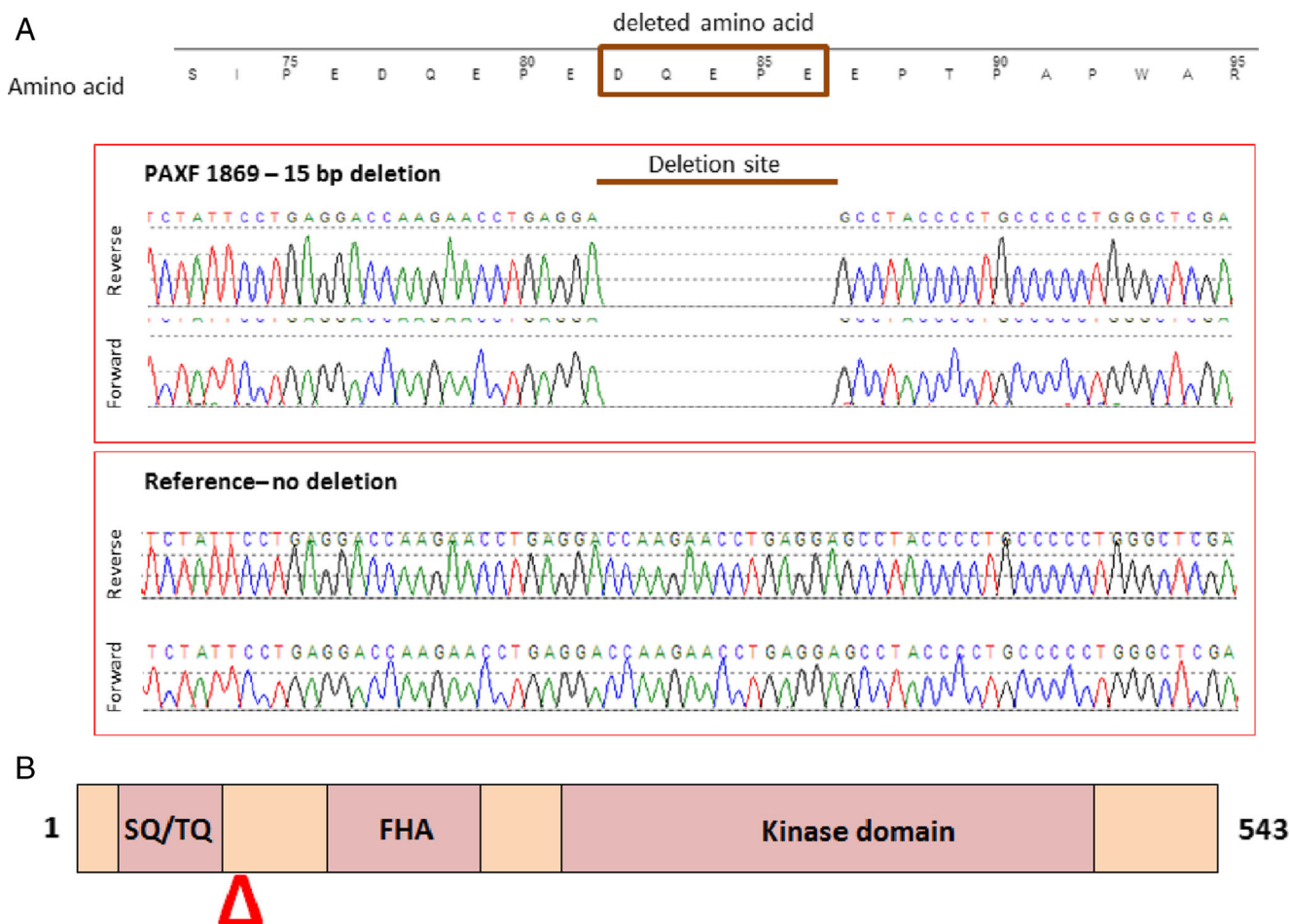


**Fig. 8** Homozygous deletion in the protein coding region of CHEK2. An in-frame deletion of codons 82–86 was detected in the first exon of CHEK2 by exome sequencing and confirmed by Sanger sequencing of amplified PCR product. **(a)** The peptide sequence of the deleted amino acids is shown aligned with the DNA sequencing readout from PCR amplified CHEK2 genomic DNA from PAXF 1869 and a reference

genome. **(b)** A schematic view of the CHK2 protein kinase showing discrete domains; the SQ/TQ region of CHK2 (aa 20–75) is a phosphorylated regulatory domain, FHA is a fork head-associated domain involved in phosphoprotein binding, and a C-terminal protein serine-threonine kinase catalytic domain

responsive *in vivo* as the HT-29 model. Both models demonstrated significant tumor growth delay when LY2603618 was administered 24 h after high-dose gemcitabine on a 3 day cycle. However, only HT-29 xenografts demonstrated significant tumor growth inhibition when mid-dose gemcitabine was dosed weekly followed 24 h later with LY2603618. The reason for the difference in combination efficacy between the two models may be due to differences in DNA damage repair or checkpoint regulation. The optimal combination schedule in the HT-29 xenograft model is to give a single dose of LY2603618 24 h following gemcitabine administration. This suggests that optimum efficacy is linked to abrogation of the S-phase DNA damage checkpoint by LY2603618 following replication collapse by gemcitabine and that long term checkpoint suppression is unnecessary.

Patient-derived tumor xenografts that are passaged only through host mice retain many of the properties of the patient's original tumor, such as morphology, microenvironment and

drug sensitivity [19]. Because of this, patient-derived tumor xenografts are thought to provide a superior evaluation of an experimental drug's ability to affect tumor growth. We observed that the patient-derived pancreatic xenograft, PAXF 1869, was only marginally affected by single agent gemcitabine or LY2603618 treatment but showed partial regression and a durable response when used in combination. The responsiveness of PAXF 1869 was surprising in light of the fact that it does not contain mutations in TP53. However, a 15 base pair in-frame deletion was found in the CHEK2 gene (aa 82–86) that could impair p53 pathway function. A mutation within this region resulting in a missense change of proline 85 to leucine has been previously identified as a somatic change in osteosarcoma and non-small cell lung cancer [41]. While it is beyond the scope of this study to investigate the functional consequences of the CHK2 aa 82–86 deletion, CHK2 does contribute to the p53-dependent G1/S checkpoint through phosphorylation of p53 on serine 20 [42].

CHK1 inhibitors have continued into the clinic to test their utility as chemopotentiators in human cancer [43]. Entering into clinical trials in 2007, LY2603618 was one of the first selective CHK1 inhibitors to be tested in patients [16]. The 24 h dosing offset suggested in this report was advanced in clinical testing in a Phase 1/2 study evaluating the combination of LY2603618 and gemcitabine in pancreatic cancer patients (NCT00839332) [18]. The observed exposures exceeded those predicted to be needed to exert biological effects in *in vivo* xenograft models. LY2603618 administered in combination with gemcitabine demonstrated an acceptable safety profile and objective responses. Although the development of LY2603618 has since been discontinued, the availability of data describing its preclinical activity benefits the clinical development of later generation CHK1 inhibitors.

**Acknowledgments** We would like to recognize the essential contributions of the original CHK1 biology and medicinal chemistry team members formerly located at Icos Pharmaceuticals: Phyllis Goldman, Erik Christenson, Darcey Clark, Jeff Dantzer, Frank Diaz, Heather Douanpanya, Francine Farouz, Ryan Holcomb, Angela Judkins, Adam Kashishian, Ed Kesicki, Kim McCaw, Harch Ooi, Vanessa Rada, Fuqiang Ruan, Alex Rudolf, Frank Stappenbeck, Janelle Taylor, Gene Thorsett, Jen Treiberg, Margaret Weidner and Steve White. We would also like to thank Steven Bray for DNA sequencing and analysis as well as Eric Westin and Aimee Bence Lin for intellectual input.

#### Compliance with ethical standards

**Conflict of interest** The authors, Darlene Barnard, H. Bruce Diaz, Teresa Burke, Gregory Donoho, Richard Beckmann, Bonita Jones, David Barda, Constance King and Mark Marshall are all employees of the Eli Lilly Company, which supports the development of LY2603618.

## References

- Patil M, Pabla N, Dong Z (2013) Checkpoint kinase 1 in DNA damage response and cell cycle regulation. *Cell Mol Life Sci: CMLS* 70(21):4009–4021. doi:10.1007/s00018-013-1307-3
- Taylor WR, Stark GR (2001) Regulation of the G2/M transition by p53. *Oncogene* 20(15):1803–1815. doi:10.1038/sj.onc.1204252
- Dai Y, Grant S (2010) New insights into checkpoint kinase 1 in the DNA damage response signaling network. *Clin Cancer Res: Off J Am Assoc Cancer Res* 16(2):376–383. doi:10.1158/1078-0432.CCR-09-1029
- Nam EA, Cortez D (2011) ATR signalling: more than meeting at the fork. *Biochem J* 436(3):527–536. doi:10.1042/BJ20102162
- Huang P, Chubb S, Hertel LW, Grindley GB, Plunkett W (1991) Action of 2',2'-difluorodeoxycytidine on DNA synthesis. *Cancer Res* 51(22):6110–6117
- Koh SB, Courtin A, Boyce RJ, Boyle RG, Richards FM, Jodrell DI (2015) CHK1 inhibition synergizes with gemcitabine initially by destabilizing the DNA replication apparatus. *Cancer Res* 75(17):3583–3595. doi:10.1158/0008-5472.CAN-14-3347
- Maity A, McKenna WG, Muschel RJ (1994) The molecular basis for cell cycle delays following ionizing radiation: a review. *Radiother Oncol: J Eur Soc Ther Radiol Oncol* 31(1):1–13
- Walworth N, Davey S, Beach D (1993) Fission yeast chk1 protein kinase links the rad checkpoint pathway to cdc2. *Nature* 363(6427):368–371. doi:10.1038/363368a0
- Zhang Y, Hunter T (2014) Roles of Chk1 in cell biology and cancer therapy. *Int J Cancer J Int Cancer* 134(5):1013–1023. doi:10.1002/ijc.28226
- Carrassa L, Damia G (2011) Unleashing Chk1 in cancer therapy. *Cell Cycle* 10(13):2121–2128
- Ewald B, Sampath D, Plunkett W (2007) H2AX phosphorylation marks gemcitabine-induced stalled replication forks and their collapse upon S-phase checkpoint abrogation. *Mol Cancer Ther* 6(4):1239–1248. doi:10.1158/1535-7163.MCT-06-0633
- Toledo LI, Altmeyer M, Rask MB, Lukas C, Larsen DH, Povlsen LK, Bekker-Jensen S, Mailand N, Bartek J, Lukas J (2013) ATR prohibits replication catastrophe by preventing global exhaustion of RPA. *Cell* 155(5):1088–1103. doi:10.1016/j.cell.2013.10.043
- Sakurikar N, Eastman A (2015) Will targeting Chk1 have a role in the future of cancer therapy? *J Clin Oncol: Off J Am Soc Clin Oncol* 33(9):1075–1077. doi:10.1200/JCO.2014.60.0767
- Walton MI, Eve PD, Hayes A, Henley AT, Valenti MR, De Haven Brandon AK, Box G, Boxall KJ, Tall M, Swales K, Matthews TP, McHardy T, Lainchbury M, Osborne J, Hunter JE, Perkins ND, Aherne GW, Reader JC, Raynaud FI, Eccles SA, Collins I, Garrett MD (2015) The clinical development candidate CCT245737 is an orally active CHK1 inhibitor with preclinical activity in RAS mutant NSCLC and Emicro-MYC driven B-cell lymphoma. *Oncotarget*
- Massey AJ, Stokes S, Browne H, Foloppe N, Fiumana A, Scrace S, Fallowfield M, Bedford S, Webb P, Baker L, Christie M, Drysdale MJ, Wood M (2015) Identification of novel, *in vivo* active Chk1 inhibitors utilizing structure guided drug design. *Oncotarget*
- Weiss GJ, Donehower RC, Iyengar T, Ramanathan RK, Lewandowski K, Westin E, Hurt K, Hynes SM, Anthony SP, McKane S (2013) Phase I dose-escalation study to examine the safety and tolerability of LY2603618, a checkpoint 1 kinase inhibitor, administered 1 day after pemetrexed 500 mg/m<sup>2</sup> every 21 days in patients with cancer. *Investig New Drugs* 31(1):136–144. doi:10.1007/s10637-012-9815-9
- Calvo E, Chen VJ, Marshall M, Ohnmacht U, Hynes SM, Kumm E, Diaz HB, Barnard D, Merzoug FF, Huber L, Kays L, Iversen P, Calles A, Voss B, Lin AB, Dickgreber N, Wehler T, Sebastian M (2014) Preclinical analyses and phase I evaluation of LY2603618 administered in combination with pemetrexed and cisplatin in patients with advanced cancer. *Investig New Drugs* 32(5):955–968. doi:10.1007/s10637-014-0114-5
- Doi T, Yoshino T, Shitara K, Matsubara N, Fuse N, Naito Y, Uenaka K, Nakamura T, Hynes SM, Lin AB (2015) Phase I study of LY2603618, a CHK1 inhibitor, in combination with gemcitabine in Japanese patients with solid tumors. *Anti-Cancer Drugs* 26(10):1043–1053. doi:10.1097/CAD.0000000000000278
- Tentler JJ, Tan AC, Weekes CD, Jimeno A, Leong S, Pitts TM, Arcaroli JJ, Messersmith WA, Eckhardt SG (2012) Patient-derived tumour xenografts as models for oncology drug development. *Nat Rev Clin Oncol* 9(6):338–350. doi:10.1038/nrclinonc.2012.61
- King C, Diaz H, Barnard D, Barda D, Clawson D, Blosser W, Cox K, Guo S, Marshall M (2014) Characterization and preclinical development of LY2603618: a selective and potent Chk1 inhibitor. *Investig New Drugs* 32(2):213–226. doi:10.1007/s10637-013-0036-7
- Merriman RL, Hertel LW, Schultz RM, Houghton PJ, Houghton JA, Rutherford PG, Tanzer LR, Boder GB, Grindley GB (1996) Comparison of the antitumor activity of gemcitabine and ara-C in



- a panel of human breast, colon, lung and pancreatic xenograft models. *Investig New Drugs* 14(3):243–247
22. Low J, Shuguang H, Dowless M, Blosser W, Vincent T, Davis S, Hodson J, Koller E, Marcusson E, Blanchard K, Stancato L (2007) High-content imaging analysis of the knockdown effects of validated siRNAs and antisense oligonucleotides. *J Biomol Screen* 12(6): 775–788. doi:10.1177/1087057107302675
  23. Li H, Durbin R (2009) Fast and accurate short read alignment with Burrows-Wheeler transform. *Bioinformatics* 25(14):1754–1760. doi:10.1093/bioinformatics/btp324
  24. Li H, Handsaker B, Wysoker A, Fennell T, Ruan J, Homer N, Marth G, Abecasis G, Durbin R (2009) The sequence alignment/map format and SAMtools. *Bioinformatics* 25(16):2078–2079. doi:10.1093/bioinformatics/btp352
  25. DePristo MA, Banks E, Poplin R, Garimella KV, Maguire JR, Hartl C, Philippakis AA, del Angel G, Rivas MA, Hanna M, McKenna A, Fennell TJ, Kernysky AM, Sivachenko AY, Cibulskis K, Gabriel SB, Altshuler D, Daly MJ (2011) A framework for variation discovery and genotyping using next-generation DNA sequencing data. *Nat Genet* 43(5):491–498. doi:10.1038/ng.806
  26. Garrison E, Marth G (2012) Haplotype-based variant detection from short-read sequencing. arXiv:12073907v2 [q-bioGN]
  27. Hui YF, Reitz J (1997) Gemcitabine: a cytidine analogue active against solid tumors. *Am J Health-Syst Pharm : AJHP : Off J Am Soc Health-Syst Pharm* 54(2):162–170, quiz 197–168
  28. Montano R, Thompson R, Chung I, Hou H, Khan N, Eastman A (2013) Sensitization of human cancer cells to gemcitabine by the Chk1 inhibitor MK-8776: cell cycle perturbation and impact of administration schedule in vitro and in vivo. *BMC Cancer* 13: 604. doi:10.1186/1471-2407-13-604
  29. Leung-Pineda V, Ryan CE, Piwnica-Worms H (2006) Phosphorylation of Chk1 by ATR is antagonized by a Chk1-regulated protein phosphatase 2A circuit. *Mol Cell Biol* 26(20): 7529–7538. doi:10.1128/MCB.00447-06
  30. Karnitz LM, Flatten KS, Wagner JM, Loegering D, Hackbarth JS, Arlander SJ, Vroman BT, Thomas MB, Baek YU, Hopkins KM, Lieberman HB, Chen J, Cliby WA, Kaufmann SH (2005) Gemcitabine-induced activation of checkpoint signaling pathways that affect tumor cell survival. *Mol Pharmacol* 68(6):1636–1644. doi:10.1124/mol.105.012716
  31. Eriksson S, Graslund A, Skog S, Thelander L, Tribukait B (1984) Cell cycle-dependent regulation of mammalian ribonucleotide reductase. The S phase-correlated increase in subunit M2 is regulated by de novo protein synthesis. *J Biol Chem* 259(19):11695–11700
  32. Del Nagro CJ, Choi J, Xiao Y, Rangell L, Mohan S, Pandita A, Zha J, Jackson PK, O'Brien T (2014) Chk1 inhibition in p53-deficient cell lines drives rapid chromosome fragmentation followed by caspase-independent cell death. *Cell Cycle* 13(2):303–314. doi:10.4161/cc.27055
  33. Tao ZF, Lin NH (2006) Chk1 inhibitors for novel cancer treatment. *Anti Cancer Agents Med Chem* 6(4):377–388
  34. Tang J, Erikson RL, Liu X (2006) Checkpoint kinase 1 (Chk1) is required for mitotic progression through negative regulation of polo-like kinase 1 (Plk1). *Proc Natl Acad Sci U S A* 103(32): 11964–11969. doi:10.1073/pnas.0604987103
  35. Parsels LA, Morgan MA, Tanska DM, Parsels JD, Palmer BD, Booth RJ, Denny WA, Canman CE, Kraker AJ, Lawrence TS, Maybaum J (2009) Gemcitabine sensitization by checkpoint kinase 1 inhibition correlates with inhibition of a Rad51 DNA damage response in pancreatic cancer cells. *Mol Cancer Ther* 8(1):45–54. doi:10.1158/1535-7163.MCT-08-0662
  36. Morgan MA, Parsels LA, Parsels JD, Mesiwala AK, Maybaum J, Lawrence TS (2005) Role of checkpoint kinase 1 in preventing premature mitosis in response to gemcitabine. *Cancer Res* 65(15): 6835–6842. doi:10.1158/0008-5472.CAN-04-2246
  37. Matthews DJ, Yakes FM, Chen J, Tadano M, Bornheim L, Clary DO, Tai A, Wagner JM, Miller N, Kim YD, Robertson S, Murray L, Karnitz LM (2007) Pharmacological abrogation of S-phase checkpoint enhances the anti-tumor activity of gemcitabine in vivo. *Cell Cycle* 6(1):104–110
  38. Ross WE, Bradley MO (1981) DNA double-stranded breaks in mammalian cells after exposure to intercalating agents. *Biochim Biophys Acta* 654(1):129–134
  39. Gonzalez Besteiro MA, Gottifredi V (2015) The fork and the kinase: a DNA replication tale from a CHK1 perspective. *Mutat Res Rev Mutat Res* 763:168–180. doi:10.1016/j.mrrev.2014.10.003
  40. Juan G, Traganos F, James WM, Ray JM, Roberge M, Sauve DM, Anderson H, Darzynkiewicz Z (1998) Histone H3 phosphorylation and expression of cyclins A and B1 measured in individual cells during their progression through G2 and mitosis. *Cytometry* 32(2): 71–77
  41. Miller CW, Ikezoe T, Krug U, Hofmann WK, Tavor S, Vegesna V, Tsukasaki K, Takeuchi S, Koeffler HP (2002) Mutations of the CHK2 gene are found in some osteosarcomas, but are rare in breast, lung, and ovarian tumors. *Genes Chromosome Cancer* 33(1):17–21
  42. Ahn J, Urist M, Prives C (2004) The Chk2 protein kinase. *DNA Repair* 3(8–9):1039–1047. doi:10.1016/j.dnarep.2004.03.033
  43. Chen T, Stephens PA, Middleton FK, Curtin NJ (2012) Targeting the S and G2 checkpoint to treat cancer. *Drug Discov Today* 17(5–6):194–202. doi:10.1016/j.drudis.2011.12.009